Reprints from
ENERGY, STRUCTURE AND REACTIVITY
Edited by Darwin W. Smith and Walter B. McRae

PHOTODETACHMENT OF NEGATIVE IONS

W. C. Lineberger†

Joint Institute for Laboratory Astrophysics and
Department of Chemistry, University of Colorado,
Boulder, Colorado 80302

I. INTRODUCTION

The vastly increased wavelength resolution at kilowatt pulse powers obtainable with continuously tunable dye lasers compared to conventional light sources affords a unique opportunity to make precise threshold measurements [1] in photodetachment of negative ions. For example, one can determine electron affinities of atomic ions to an accuracy of 10-100 times greater than that which can be obtained [2] with conventional blackbody light sources. In addition, the high resolution (better than 1Å) enables one to study the threshold behavior cross section, obtaining information on the range of validity of various threshold expansions which was not previously available. In this paper I will attempt to describe briefly a tunable laser photodetachment apparatus, the current status of threshold photodetachment theory and recent tunable laser photodetachment data for atomic and molecular ions. The difficulties involved in interpreting the molecular ion photodetachment data will lead us naturally to consider the possibility of multiphoton photodetachment and photodissociation as an alternative means of obtaining negative ion structure information. Comparisons with theoretical results will be made where appropriate. Finally, some conservative predictions will be made concerning experiments that are possible with straightforward extensions of today's technology. It is hoped that this paper will raise at least as many questions as it answers for it is the author's prejudiced opinion that there are many exciting new experiments and calculations remaining to be done in the field of negative ion structure and properties.

---

†Alfred P. Sloan Foundation Fellow, 1972-74.

II. EXPERIMENTAL APPARATUS

A schematic diagram of a typical tunable laser photodetachment machine is shown in Fig. 1. The basic idea is to intersect a several kilovolt mass analyzed negative ion beam with the focused output of a pulsed tunable dye laser and to measure the relative cross section for production of neutral atoms as a function of the laser wavelength. The negative ions are formed in the ion source, which is typically either a hot cathode arc discharge [3] or, if one is interested in refractory metal negative ions, a sputtering discharge [4]. Upon extraction from the ion source, the ions are accelerated to several kilovolts, mass analyzed, and focused onto a 15-stage particle multiplier located 20 cm beyond the laser beam intersection region. Beyond the intersection region but before reaching the multiplier, the ions are electrostatically deflected into a Faraday cup, so that only the neutral atoms, produced by charge-stripping on the background gas and by laser photodetachment, reach the neutral detector. As a result of the large number of neutrals reaching the multiplier in a short time interval, the detector is operated in a linear, charge-amplifying mode, rather than as a particle counter.

The light source is a flash lamp pumped, tunable organic dye laser [5] consisting of a linear xenon flash lamp and a dye cell located at the foci of an elliptical cavity. Wavelength selection is achieved with the use of an 1800 ℓ/mm diffraction grating, blazed at 5000 Å in first order, as one feedback element in the laser optical cavity. A partially transmitting mirror serves as the output coupler. The laser output is a 300 nsec pulse, with an energy content of 1-5 mJ per pulse and a line width typically 1 to 2 Å. The laser used in

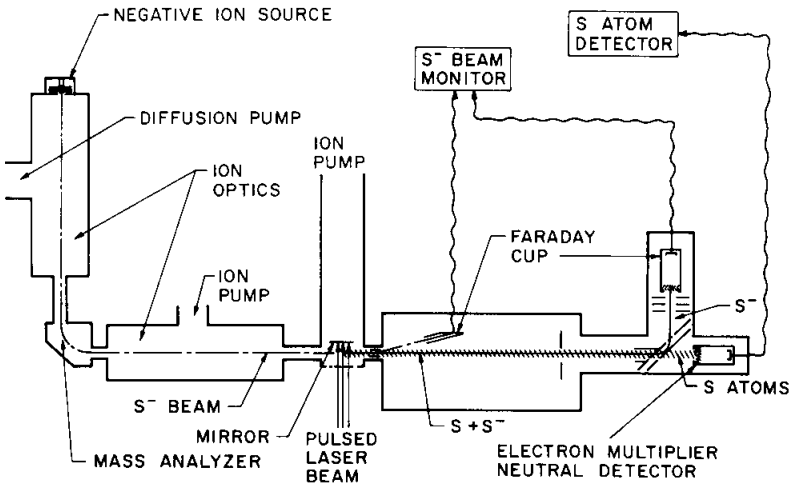

Fig. 1. Diagram of a tunable laser photodetachment apparatus.

these experiments was tunable over the wavelength range 4500 - 7000 Å by proper selection of laser dyes. Typical repetition rates were 5 Hz.

The pulsed laser beam is focused onto the negative ion beam and the neutral particle multiplier is gated on after a delay following the laser pulse appropriate to the neutral flight time from the interaction region to the detector. The neutral detector is also gated on to sample the stripped neutral signal approximately 1 μsec before the laser produced neutrals reach the multiplier, thus providing a neutral background correction obtained in a time short compared to the coherence time of the negative ion beam. A small portion of the laser beam is detected by a fast photodiode, and another gate samples the ion beam current at the time of laser firing. A small computer is utilized to control the wavelength of the laser, acquire the various signals, and compute the relative neutral production cross section from the various signals. A 0.35 m monochrometer, accurate to better than ±1 Å is used to measure the laser wavelength and line width.

As a result of the intense laser pulse and the relatively low background pressures in the interaction region (approximately 10^{-8} torr), the signal-to-noise ratio is quite high in these measurements and it is, in principle, possible to measure cross sections as small as 10^{-24} cm^2 with a signal-to-noise ratio of 10 in a 100 laser shot integration period. It is important to note that what is actually measured is a cross section for production of neutral atoms which, in general, is the sum of photodetachment and photodissociation cross sections. If a photodissociation channel is open, one needs additional information to extract the photodetachment portion of the neutral production cross section.

III. THEORETICAL BACKGROUND

In this section we will briefly review what is theoretically known about the threshold behavior of photodetachment cross sections. As for many other processes, the starting point is the classic paper by Wigner [6] on the threshold energy dependence of processes in which pairs of particles are formed. He derives the general result

$$\sigma \propto k^{2L+1} \propto (E-E_{thr})^{\frac{2L+1}{2}} \qquad (1)$$

for the case in which the final state interactions (other than the centrifugal potential) fall off faster than $1/r^2$. In the case of photodetachment, k is very close to the electron momentum and L is its orbital angular momentum with respect to the atom.

O'Malley [7] has investigated the influence of long-range potentials on the photodetachment cross section near threshold. When he

included the electron-induced dipole (r^{-4}) interaction in the final state he obtained

$$\sigma \propto (h\nu)k^{2L+1}\left[1 - \frac{4\alpha k^2 \ell nk}{a_o(2L+3)(2L+1)(2L-1)} + O(k^2)\right] \qquad (2)$$

where $h\nu$ is the photon energy, α is the dipole polarizability of the final state atom, e is the unit of electronic charge, a_o is the Bohr radius, α and k are in atomic units and $O(k^2)$ represents terms of order k^2 and higher.

It is interesting to note that this new correction term is negative for $L = 0$, whereas it is positive for $L > 0$ (only $k << 1$ is considered). This result is qualitatively understood by noting that the polarization potential, which is always attractive, decreases the centrifugal barrier for $L > 0$ resulting in an increased cross section; on the other hand, for $L = 0$ the leaving electron is "reattracted" to the atom leading to a decrease in the cross section. The basic idea in O'Malley's treatment, which is based on the modified effective range theory (MERT) developed by O'Malley, Spruch and Rosenberg [8] is that the major energy dependence of the correction term originates in the energy dependence of the normalization factor to the radial wavefunction. If the latter is chosen to be energy independent at small distances (where the matrix element is evaluated), it is then possible to extend O'Malley's treatment, if one assumes that the terms of $O(k^2)$ which come from the matrix element squared can be neglected in comparison with those originating from the normalization factor. If one carries out the expansion of the normalization factor to include explicitly terms of order k^2 and k^3 in MERT then one obtains [3] the following expression for the threshold photodetachment cross section for the simplest case of $L = 0$:

$$\sigma \propto (h\nu)k\left[1 + \frac{4}{3}\beta^2k^2\ell n\ 1.23\ \beta k + Ak^2\left(r_{p_o} + \frac{2\pi}{3}\beta - A\right) + \frac{4\pi}{3}\beta^2Ak^3\right] \qquad (3)$$

where $\beta^2 = \alpha/a_o$, A is the scattering length, and r_{po} is the modified effective range.

We note that all of the parameters that are used to describe low-energy electron-atom elastic scattering appear in this formula. This has to do with the fact that photodetachment can be viewed as "half an elastic scattering process," and, near threshold, modified effective range theory may be applied. This expression (3) is valid only if the following conditions are met:

(1) The energy dependence of the square of the matrix element is small compared to the one given in Eq. (3).

(2) The atom A is in a state with $J = 0$.
(3) βk (i.e., the expansion parameter in MERT) $<< 1$.

With these restrictions one can attempt to fit, near threshold, photodetachment data to this expression in order to obtain elastic scattering information. It is quite clear that such information is contained in the departures from the Wigner threshold law, but it is not at all clear that this approach is the best way to extract that information.

While the threshold law for photodetachment of atomic negative ions is relatively well understood, essentially nothing is known about the threshold law for individual rotational transitions in photodetachment of molecular negative ions possessing a permanent electric dipole moment. Geltman [9] has predicted the threshold behavior for molecular photodetachment in the case of short-ranged potentials, but does not consider the effect of a permanent electric dipole moment. The influence of the long-range electron permanent dipole interaction (proportional to $1/r^2$) can be expected to change the basic energy dependence for sufficiently large permanent dipole moments. O'Malley [7] has treated the electron plus $H(n = 2)$ as an example of an electron-dipole interaction. The difference compared to the molecular dipole case is the feature that in the $H(n = 2)$ case the "atomic dipole" is always directed toward the departing electron so that the interaction energy does not contain the complicating angular dependence. It must be stressed that one expects the threshold behavior to be a function of the rotational energy of the negative ion, since the effects of the rotation of the dipole field will be different for slow and fast rotation. For example, one can show [10] that in the case of photodetachment of OH^-, the rotation of the permanent dipole can be neglected near threshold only for the very lowest rotational states. A considerable amount of theoretical work is required to understand the molecular photodetachment thresholds.

IV. ATOMIC NEGATIVE IONS

Experimentally the simplest case to study is photodetachment of an atomic negative ion in which the outer electron is in a p shell. In this case the Wigner threshold law predicts that the cross section is proportional to the square root of the excess energy and leads to the delightful case of an infinite derivative at threshold. What one expects to see in detail is indicated in Fig. 2, which shows an energy-level diagram for Se^- and Se. We thus expect to see a series of $E^{1/2}$ thresholds corresponding to some or all of the six possible fine structure transitions from $^2P_{1/2,3/2}$ Se^- to the $^3P_{2,1,0}$ Se final states. If we observe all of these transitions, then the proper identification becomes trivial because the neutral

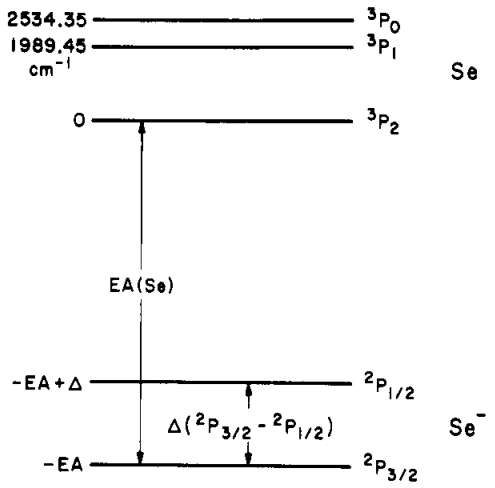

Fig. 2. Energy level diagram of Se and Se^-.

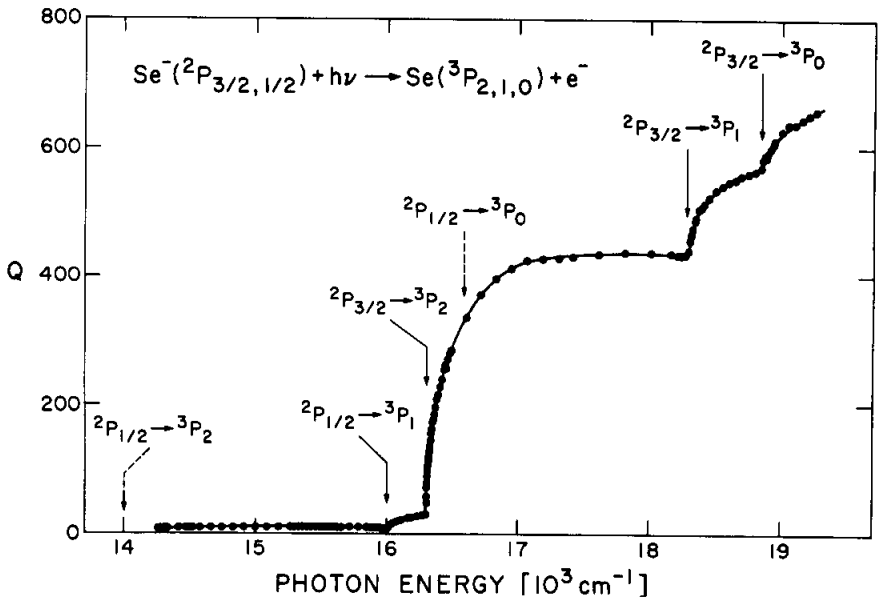

Fig. 3. Se^- photodetachment cross section in the energy range 14,000-19,000 cm^{-1}. The individual fine structure transition thresholds are labeled (see text for details).

spin-orbit splittings are well known from conventional spectroscopy. Figure 3 shows the experimental results for photodetachment of Se^- obtained [3] with the apparatus described previously. The appropriate transitions are labeled on the figure. From these data we immediately deduce that the electron affinity of selenium is 2.0204 ± 0.0004 eV, and that the spin orbit splitting in Se^- is 2279 ± 2 cm^{-1}. Figure 4 is a plot of the cross section as a function of electron momentum for just the $^2P_{3/2} - {}^3P_2$ partial cross section. Note that the Wigner threshold law is valid for only the first 5 meV above threshold. If we set $\alpha = 30\ a_o^3$, $r_{p_o} = 0$, ignore the electron - quadrupole interaction, and attempt to fit these data to Eq. (3), we obtain a scattering length of approximately $-6a_o$. The significance of such a fit, however, is not at all obvious.

Since we can show that the Wigner threshold law is valid for some range near threshold, we can now experimentally determine the relative strengths of the various fine structure transitions. Such

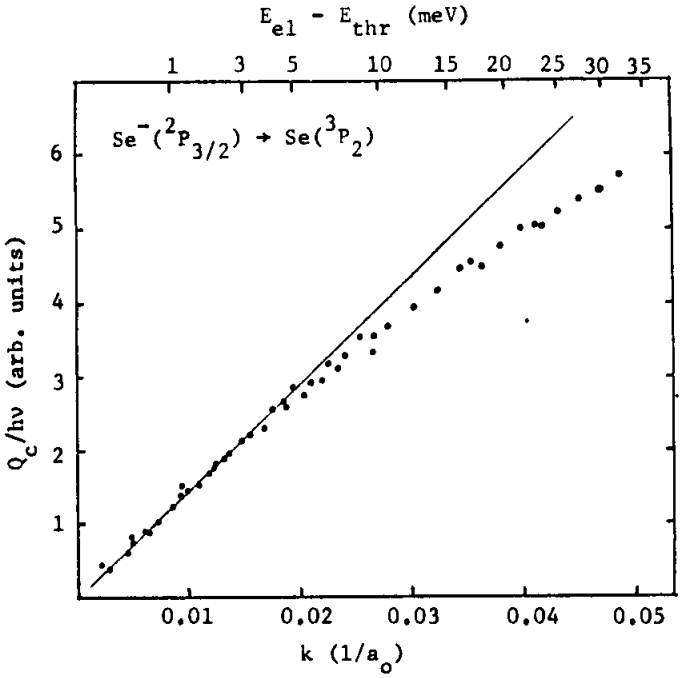

Fig. 4. $Se^- {}^2P_{3/2} - Se\ {}^3P_2$ partial photodetachment cross section plotted as a function of electron momentum in atomic units. The straight line is the Wigner threshold law, which appears to be valid for only the first 5 meV above threshold.

data make it clear that it is necessary to view the final state in the detachment process as a complex (e + atom) in LS-coupling and then study how this complex breaks up into jj-coupled fragments [1]. Since this process has been discussed in detail [11] elsewhere, it will not be pursued further here.

Having established the validity of the Wigner threshold law for the case of the bound p electron, one would like to look at the case of photodetachment of a bound s electron. Given the range of photon energies available from our tunable dye laser, the most promising candidate appeared to be gold. A plot of the Au^- photodetachment data [4] is shown in Fig. 5. Since the Wigner threshold law predicts that the cross section is proportional to (excess energy)$^{3/2}$, a plot of the Au^-(cross section)$^{2/3}$ as a function of photon energy should be a straight line. That this result is obtained is shown in Fig. 6. From an analysis of these data we find that EA(Au) = 2.3086 ± 0.0007 eV. In the case of gold the Wigner threshold law is valid for nearly 60 meV, in sharp contrast with the selenium case; this result is due to the fact that the two dominant higher order correction terms to the cross sections are of approximately equal magnitude and happen to go in opposite directions. Similar measurements on platinum [4] showed that the electron affinity of platinum was 2.128 ± 0.002 eV.

When such measurements were attempted for silver and copper ions, whose electron affinities had been estimated via surface ionization techniques [12,13] to lie within the range accessible to our dye laser, we found strong detachment signals at the reddest wavelengths available to us. Consequently, in order to be able to measure these electron affinities, it was necessary to utilize the laser photoelectron spectroscopy apparatus developed by J. L. Hall and his colleagues [14-16]. In this apparatus a negative ion beam is crossed by a fixed wavelength argon ion laser and the energy distributions of the ejected electrons are measured. From such measurements we find [7] that EA(Cu) = 1.226 ± 0.010 eV and EA(Ag) = $1.303 \pm \begin{matrix} 0.007 \\ 0.011 \end{matrix}$ eV. These electron affinities are all approximately 0.5 eV less than those determined by surface ionization studies and clearly indicate that some of the assumptions made in the analysis of surface ionization data are not always met. A summary of electron affinity determinations for copper, silver and gold appears in Table 1. In the case of copper, there have been two theoretical determinations [18,19] of electron affinities, both of which are substantially in error. This result simply indicates the difficulty of accurate electron affinity calculations for large atomic systems. Consequently, the method of isoelectronic extrapolation [20,21] (which empirically accounts for the effects which make accurate calculations so difficult) may provide the best estimates for the electron affinities of heavy elements, especially if reliable benchmarks are used in the extrapolation. In particular, one can estimate the electron affinities of the

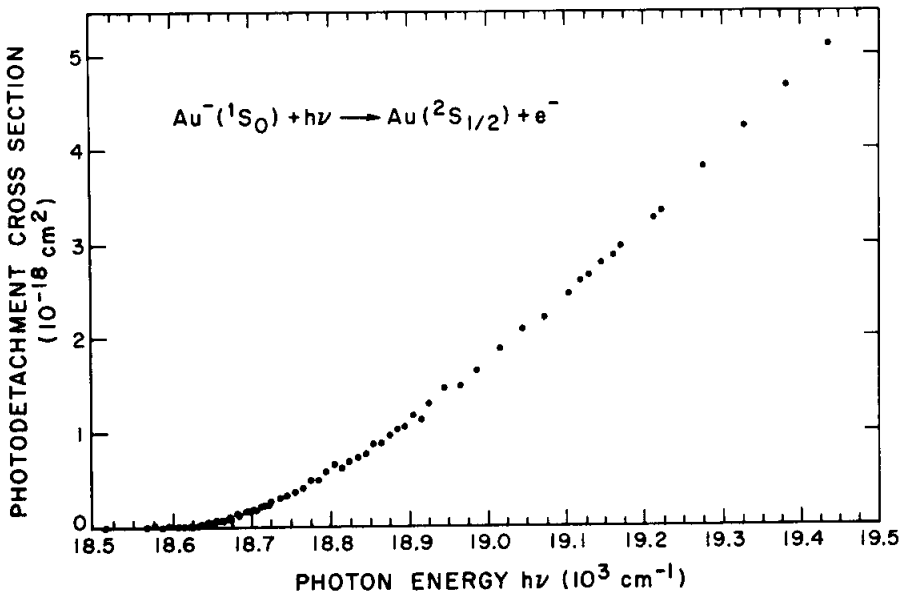

Fig. 5. Au^- photodetachment cross section.

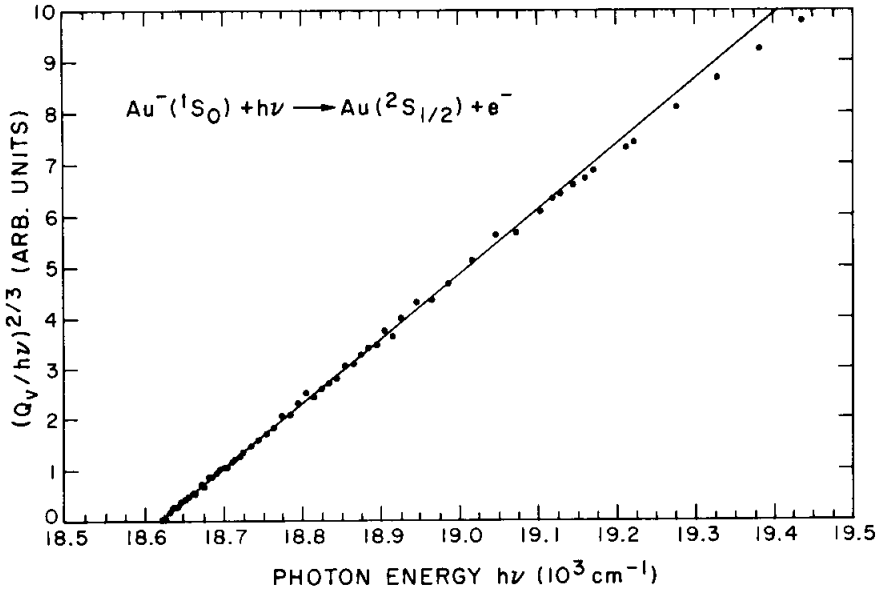

Fig. 6. Plot of $(Q/h\nu)^{2/3}$ vs photon energy $h\nu$ in the range 18,500-19,500 cm^{-1} with Q being the photodetachment cross section of Au^-. Straight line behavior corresponds to the Wigner threshold law.

Table 1

Electron affinities of Cu, Ag, and Au in electron volts

Author	Reference	Method	Cu	Ag	Au
Bakulina, Ionov	12	Relative surface ionization	1.5 ± 0.5	2.0 ± 0.2	2.8 ± 0.1
Zandberg et al.	13a	Absolute surface ionization	----	1.90 ± 0.15	----
Zandberg et al.	13b	Relative surface ionization	EA(Ag) - 0.12 ± 0.06	----	----
Hotop, Lineberger	4	Photodetachment	----	$\lesssim 1.5$	2.3086 ± 0.0007
Hotop et al.	17	Photodetached electron spectroscopy	1.226 ± 0.010	$1.303 \begin{smallmatrix} + 0.007 \\ - 0.011 \end{smallmatrix}$	----
Clementi	19	Hartree-Fock calculation	1.80 ± 0.1	----	----
Schwarz	18	Pseudopotential calculation	0.7	----	----
Charkin, Dyatkina	20	Isoelectronic extrapolation	1.4	1.5	----

elements in the three long series (K → Cu, Rb → Ag, Cs → Au) via horizontal isoelectronic extrapolations.

Charkin and Dyatkina [20] and Zollweg [21] have shown that the energy difference between the two configurations $d^K s^2$ and $d^K s$ (K = 0, ···, 10) increases nearly linearly with K. Since it is well established [20] that the ground state configuration of negative ions in the three long periods is $d^K s^2$, one can estimate the electron affinities of these atoms if those for K, Rb, and Cs on the one side, and those for Cu, Ag, and Au on the other side are known, because then the slope of the straight line representing the $d^K s^2 \rightarrow d^K s$ energy differences between the negative ion and the $d^K s$ neutral atom state is fixed.

For this extrapolation we use the noble metal electron affinities measured by us and for the alkalis we use the electron affinities calculated by Weiss. The results obtained [17] from this extrapolation are shown in Table 2 and represent our best estimate of the electron affinities of the unmeasured elements of the three long series.

V. MOLECULAR NEGATIVE IONS

As a result of the manifold of rotational transitions involved and the fact that the exact form of the threshold law is both unknown and rotational energy dependent, one can confidently predict that the detailed interpretation of molecular ion photodetachment data will be very difficult. Perhaps the simplest case one can consider is photodetachment of OH^-, for which it has been established [22-24] that r_e is virtually the same for the negative ion and the neutral molecule. Furthermore, one expects [7,9] that the individual thresholds will be at least as sharp as $E^{1/2}$. The general shape of the photodetachment cross section observed [10] in the range 14,275 - 15,475 cm^{-1} (7,000-6,450 Å) is shown in Fig. 7 and a more detailed view of the cross section in the region around the sharp onset is shown in Fig. 8. This onset, which essentially covers a range of 50 cm^{-1}, is due to the opening of what we shall call the Q-rotational branches for transitions from OH^- $^1\Sigma$ to OH $^2\Pi_{3/2}$. The conclusions that we have been able to reach for this ion have all been drawn from a detailed inspection of this portion of the observed cross section. The basic procedure [10] used has been to construct synthetic photodetachment cross sections based on the known spectroscopic constants of the OH molecule and the measured r_e in the negative ion. In addition, one must assume some form for the threshold law. Based on such fits we find EA(OH) = 14,723 ± 15 cm^{-1}; similar studies on OD^- yield 14,703 ± 15 cm^{-1}. The observed isotope effect (20 ± 10 cm^{-1}) for the electron affinity difference can almost entirely be ascribed

Our method for the calculation of E_r and Γ is based on the stabilization method which was originally developed by Taylor and coworkers [Advan. Chem. Phys. 18, 91 (1970)]. By studying a model problem we have provided a mathematical justification of the computational procedure [Phys. Rev. A 1, 1109 (1970); also see the work by W. Reinhardt, Phys. Rev. Letters 28, 401 (1972)]. More recently, we have proposed a practical method for the calculation of AI lifetimes [Chem. Phys. Letters 8, 582 (1971)] and extended the method to multichannel problems where the AI states can decay into several final states [Phys. Rev. A 5, 1236 (1972)].

The present version of the stabilization method can be summarized as follows. Based on the expected electron configurations of the AI states under study, one chooses an appropriate set of square-integrable many-electron basis functions (configurations) which spans the interaction region. Using the Born-Oppenheimer approximation, the electronic Hamiltonian is diagonalized in successively larger basis sets. To identify an AI state, one looks for a stable root of the energy matrix, i.e., a root which changes relatively little as the size of the basis increases and for which the corresponding eigenfunction is most localized in configuration space. We have shown that the value of the stable root is a first approximation to the energy of the AI state and that the degree of stability is inversely proportional to its lifetime. The eigenfunction corresponding to the stable root is a good approximation, apart from an overall normalization factor, to the inner part of the exact wave function of the AI state and can be used to calculate E_r and Γ. The AI lifetimes are calculated from a "Golden-Rule-like" formula involving the matrix element of the electronic Hamiltonian between the square-integrable eigenfunction and a continuum function representing the ionized state. The slowly varying (as a function of the energy) background scattering matrix, which is required to specify the continuum function, can be determined using the criterion that several good approximations to the AI state give exactly the same decay lifetime.

The stabilization method has the following advantages over other procedures: i) in contrast to methods utilizing projection operators, it is equally applicable to all types of AI states, to shape- as well as compound-state-resonances, ii) the explicit construction of many-electron projection operators is not required, iii) it gives an approximation to the exact, "shifted" energy of the AI state, and to an eigenvalue of some projected Hamiltonian QHQ, iv) it provides some information about the wave function representing the background continuum underlying the AI state. One disadvantage is the apparent lack of stationary or extremum principles associated with the method.

The overall success of the stabilization method depends critically on the nature and the extent of the basis set chosen for the calculations. In this respect, the method does differ from any other

quantum mechanical treatment of bound and unbound atomic or molecular states which utilize the expansion technique.

SESSION I

LARGE MOLECULES: AB INITIO TECHNIQUES

POSITION PAPERS

R. E. Christoffersen
Computational Techniques for Large Molecules

K. F. Freed
Completely Ab Initio Justification of Purely Semi-Empirical Theories